Available online at www.sciencedirect.com
SCIENCE DIRECT®
Biochemical and Biophysical Research Communications 331 (2005) 78–85
BBRC
www.elsevier.com/locate/ybbrc

# Induction of a SSAT isoform in response to hypoxia or iron deficiency and its protective effects on cell death ☆

Kyuheun Kim [a,1], Ji-Hye Ryu [b,1], Jong-Wan Park [b], Myung-Suk Kim [b], Yang-Sook Chun [a,*]

[a] *Department of Physiology, Cancer Research Institute, Seoul National University College of Medicine, 28 Yongon-dong, Chongno-gu, Seoul 110-799, Republic of Korea*
[b] *Department of Pharmacology, Seoul National University College of Medicine, 28 Yongon-dong, Chongno-gu, Seoul 110-799, Republic of Korea*

Received 21 March 2005
Available online 30 March 2005

**Abstract**

Spermidine/spermine $N^1$-acetyltransferase (SSAT) is the key enzyme with regard to the maintenance of intracellular polyamine levels. It is an inducible enzyme, which may participate in adaptive responses to environmental stress. However, little is known regarding its responses to oxygen or nutrient deficiencies. Using microarray assays, we discovered that SSAT was enhanced under both oxygen- and iron-deficient conditions. However, RT-PCR revealed that the SSAT mRNA was not induced; rather, an mRNA variant was newly expressed. In this variant, the splicing-in of 110 bases induces early termination, generating a truncated isoform which lacks catalytic motifs. The variant expression occurs in other cancer cells and was irrelevant to both hypoxia-inducible factor 1 and to the redox state. We attempted to determine its role, using stable cell-lines. The expressed isoform was found to promote cell survival under iron-deficient conditions and blocked the cleavage of poly(ADP–ribose) polymerase. This isoform may contribute to the progression of tumors of a more malignant phenotype under poor conditions and may constitute a potential target for anticancer therapy.


*Keywords:* Spermidine/spermine $N^1$-acetyltransferase; Polyamines; Alternative RNA splicing; Hypoxia; Desferrioxamine

Spermidine/spermine $N^1$-acetyltransferase (SSAT) is the principal catabolic enzyme responsible for the regulation of intracellular polyamine contents in mammalian cells [1]. SSAT transfers an acetyl group from acetyl-CoA to the $N^1$ positions of spermidine and spermine. The $N^1$-acetyl derivatives are excreted outwards, or are converted further by polyamine oxidase, ultimately yielding putrescine, which is a pathway opposite to that of polyamine synthesis. In addition to reducing polyamine contents, the negative-charged acetyl group can immediately inactivate polyamine functions, via the prevention of interaction with the anionic sites in nucleic acids and proteins. As polyamines are essential for cell proliferation, differentiation, and apoptosis [2], the levels of polyamines are strictly regulated via the coordination of several enzymes which synthesize and remove polyamines [3]. Therefore, SSAT might protect cells from toxicity due to overproduced polyamines and, therefore, maintain a polyamine level balance, according to the needs of the cell.

The human SSAT gene is located on the short arm of the X-chromosome at the p22.1 locus (GenBank Z14136) [4]. This gene produces the 1060 bp SSAT

☆ *Abbreviations:* DFO, desferrioxamine; HIF-1, hypoxia-inducible factor 1; SSAT, spermidine/spermine $N^1$-acetyltransferase; *is*SSAT, inducible short SSAT.

* Corresponding author. Fax: +82 2 7457996.
*E-mail address:* chunys@snu.ac.kr (Y.-S. Chun).

[1] Contributed equally to this paper.

0006-291X/$ - see front matter © 2005 Elsevier Inc. All rights reserved.
doi:10.1016/j.bbrc.2005.03.121

mRNA (GenBank NM_002970), which, in turn, translates a 171-amino acid protein. Interestingly, this gene has a very long intron 3, measuring 1449 bp. As it is quickly degraded via the ubiquitin–proteasome pathway [5], SSAT is normally present in very small amounts and is undetectable in unstimulated cells by immunoblotting. However, SSAT expression is induced at a substantial level by endogenous and environmental factors, including a variety of hormones and growth factors, toxic agents, and the polyamines themselves [1]. SSAT overexpression has been implicated in adaptive responses to environmental stress [6]. However, little remains known regarding the regulation of SSAT in response to oxygen or nutrient deficiencies.

As rapidly growing tumors consume a significant amount of oxygen and nutrients, they tend to be subjected to relative hypoxia and malnutrition [7,8]. In addition, the tumor blood supply is insufficient, as blood vessel formation is slower than tumor growth, and the aberrant tumor vessel can thus collapse or leak, thereby exacerbating the existing oxygen and nutrient deficiency [9]. In the present study, we attempted to determine the manner in which SSAT is regulated under oxygen- and iron-deficient conditions. Interestingly, we determined that a short form of SSAT was induced at high levels under such conditions, and that the isoform prevented cells from apoptotic death, regardless of polyamine metabolism. This isoform induction appears to constitute an adaptive mechanism for the survival of cancer cells under poor conditions, which implies the possibility that the isoform may constitute a target for the development of a new anticancer treatment modality.

## Materials and methods

*Materials.* Culture media and fetal bovine serum were purchased from Life Technologies (Grand Island, NY). Desferrioxamine, $CoCl_2$, MG132, and other chemicals were purchased from Sigma–Aldrich (St. Louis, MO). Rat anti-hemagglutinin (HA) monoclonal antibody were purchased from Roche Applied Science (Germany) and anti-*is*SSAT polyclonal antiserum was generated in rats, against a bacterially expressed fragment which encompassed the full length of the *is*SSAT protein (supplementary material 1).

*Cell culture.* HEK293 (embryonal kidney), Caki1 (renal cancer), HT29 (colon cancer), SiHa (uterine cervical cancer), Hep3B (liver cancer), MCF7 (breast cancer), PC3 (prostate cancer), and MKN28 (gastric cancer) were used. These cell-lines (ATCC: Manassas, VA) were cultured in modified Eagle's medium α (MEM-α) or Dulbecco's MEM (DMEM), supplemented with 10% heat-inactivated FBS, penicillin (100 U/ml), and streptomycin (100 U/ml). The cells were grown in a humidified atmosphere containing 5% $CO_2$ at 37 °C. Oxygen tension in the incubator (Vision Sci, Korea) was either 140 mmHg (20% $O_2$ v/v, for normoxia) or 7 mmHg (1% $O_2$ v/v, for hypoxia).

*RNA isolation and microarrays.* Total RNA was isolated from the HEK293 cells with TRIZOL reagent (Molecular Research Center), according to the manufacturer's protocol. The RNA pellet was then dissolved in appropriate RNase-free water, and the RNA quality was confirmed with 1% denaturing formaldehyde gel, by ensuring the presence of the 28S and 18S ribosomal bands. The human oligochip for the 11,000 cDNA was obtained from MacroGene (Seoul, Korea). From 100 μg of RNAs, the cDNA probes were synthesized using SuperScript II RT (Invitrogen, Carlsbad, CA) with an oligo(dT) primer and labeled with Cy3 or Cy5 dye (Amersham Biosciences, Piscataway, NJ). Array slides were prehybridized for 1 h and then hybridized with 40 μl of cDNA probe for 18 h. The slides were washed, scanned, and analyzed, using Genepix 3.0 software (Axon Instruments, Foster City, CA). In order to ensure the reliability of the data, each sample was also reciprocally labeled in all of the hybridization experiments.

*Identification and cloning of a SSAT variant cDNA.* Reverse transcription polymerase reaction (RT-PCR) was conducted in order to identify SSAT cDNAs [10]. One microgram of total RNA was reverse transcribed at 42 °C for 1 h, after which the cDNAs were amplified over 20 PCR cycles (94 °C for 30 s denaturing, 53 °C for 30 s annealing, and 68 °C for 30 s elongation) in a 25 μl reaction mixture containing 5 μCi [α-$^{32}$P]dCTP and 25 pmol primers. The PCR products were then electrophoresed on 4% polyacrylamide gel at 100 V in a 1× Tris/borate/EDTA (TBE) buffer, and the dried gels were then autoradiographed. The PCR products, after being electrophoresed on agarose gel, were extracted and sequenced directly. The cDNAs were cloned into pCR2.1-TOPO (Invitrogen, Carlsbad, CA) and transformed into *Escherichia coli*. The plasmid containing the full-length SSAT variant was purified, and the DNA sequence was analyzed. Primer sequences (5′ to 3′) for the identification of intron 3 insertion and for full-length SSAT cDNAs were: CTGCTAGAAGATG GTTTTGG/ACTGGACAGATCAGAAGCAC and TGGTGTTTAT CCGTCACTCGC/TTAAAAAAGAATCAAACAGAAACTC, respectively. Primer sequences for human β-actin were: AAGAGAGGCAT CCTCACCCT/ATCTCTTGCTCGAAGTCCAG. Although the SSAT variant cDNA with the intron 3 insertion was longer than that of the wild-type, it translates a shorter form of the SSAT protein. In addition, the variant can be induced by hypoxia or DFO treatment. Thus, here we designate the variant protein as "inducible short SSAT" (*is*SSAT).

*Expression plasmids and the establishment of stable cell-lines.* The cloned cDNAs of SSAT and its variant were inserted into pcDNA3 vector or into pcDNA3 vector containing the HA-tag sequence. All constructs were confirmed to be the appropriate insert via DNA sequence analysis. HEK293 cells were stably transfected with pcDNA3, pcDNA3-HA-SSAT, pcDNA3-HA-*is*SSAT, and pcDNA-*is*SSAT using the calcium phosphate method and were transfected with 10 μg DNAs on 50% confluent cells in 100-mm diameter culture dishes. After 48 h of stabilization, transfection efficiency was verified by checking the protein levels with specific antibodies. The transfected cells were then cultured in media containing 0.45 mg/ml G418, in order to select the transfected cells. Stable cell-lines obtained from four different transfections were pooled after 30 days, thereby avoiding bias with regard to gene expression due to variable chromosomal integration sites.

*Immunoblot analysis of SSAT and its variant protein.* For the detection of SSAT and its variant protein, the cells were lysed in buffer containing 200 mM Tris (PH 6.8), 2% SDS, 40% glycerol, and 10% β-mercaptoethanol. The proteins were separated on a 20% Tris/Tricine gel and transferred to a NC membrane (Protran, Schleicher & Schuell Bioscience, Germany). Membranes were blocked with 5% nonfat milk in Tris-buffered saline (TBS) containing 0.1% Tween 20 (TTBS) at room temperature for 1 h, then incubated overnight at 4 °C with anti-HA or anti-*is*SSAT, and diluted 1:5000 in 5% nonfat milk in TTBS. Horseradish peroxidase-conjugated anti-rat antiserum was utilized as a secondary antibody (1:5000 dilution in 5% nonfat milk in TTBS, 1 h incubation), and the antigen–antibody complexes were visualized with an Enhanced Chemiluminescence Plus kit (Amersham Biosciences, Piscataway, NJ). For the detection of PARP cleavage, the cells were lysed in buffer containing 50 mM Hepes (pH 7.4), 150 mM NaCl, 20 mM EDTA, 100 μM NaF, 10 mM $Na_3VO_4$, 1 mM phenylmethylsulfonyl fluoride, 1 mM leupeptin, 20 μg/ml aprotinin, and 1% Triton

X-100. The proteins were separated on 7.5% SDS–PAGE and transferred to Immobilon P (Millipore, Bedford, MA). PARP protein was detected using anti-PARP antibody (BIOMOL Research Laboratories, Plymouth Meeting, PA), and horseradish peroxidase-conjugated anti-mouse antiserum (Zymed Laboratories, South San Francisco, CA). Protein loading was controlled by probing the membranes for β-actin protein.

*Cell viability assay*. Cell viability was determined via MTT assay. Cells were plated onto 24-well plates. A MTT solution (Sigma–Aldrich) at a final concentration of 0.5 mg/ml was added to the media and then incubated at 37 °C for 3 h. The resulting insoluble formazan was then dissolved with 0.04 M HCl in isopropanol. Absorbance of the purple color of formazan was measured at 570 nm with a spectrophotometer.

*Polyamine assay*. Intracellular polyamines were extracted from cell pellets with 0.6 N perchloric acid, dansylated, and then measured via reverse phase HPLC, as previously described [11]. Dansylated samples were injected into a 250-mm × 3.2-mm internal diameter Econosil C18 column (5-μm particle size, Alltech, Deerfield, IL) with a column temperature of 50 °C, and then eluted by a two-solvent gradient using a Waters 616 LC system (Waters, Milford, MA). Solvent A contained 55% of 10 mM ammonium phosphate and 45% acetonitrile, at a pH of 4.4. Solvent B contained 100% acetonitrile. At 0.9 ml/min, the gradient began at 100% solvent A, and progressed in a linear fashion to 82% solvent B over 30 min, with a 15-min hold. Dansylated polyamines were detected using a fluorescence detector with an excitation wavelength of 360 nm. Polyamines and their acetyl forms (Sigma–Aldrich) were then dansylated and applied, in order to identify the retention time of each polyamine, and to quantify polyamine levels in samples (supplementary material 2).

*ATP assay*. The intracellular amounts of ATP were measured using the Bioluminescent Somatic Cell Assay Kit provided from Sigma. One hundred microliters of cell suspensions in PBS was added to 100 μl of the ATP releasing reagent, and mixed with 100 μl ATP assay mixture containing firefly luciferin, as described in the manufacturer's manual. The bioluminescence was monitored using the Lumat LB9507 luminometer (Berthold), and the amount of ATP was calculated by using the ATP standard solution provided from the manufacturer.

*Statistical analysis*. All data were analyzed using Microsoft Excel 2002 software (Microsoft, Redmond, WA). Data are expressed as means and SD values. Student's $t$ tests were used to analyze statistical differences, which were considered significant when $p < 0.05$.

## Results and discussion

As tumors tend to eventually outgrow their blood supply, hypoxia and poor nutrition are characteristic features of rapidly growing solid tumors. Such conditions promote genomic instability through point mutations, gene amplification, and chromosomal rearrangement, leading to the activation of oncogenes or the inactivation of tumor suppressor genes [12]. Once the genetic alterations become favorable for cell survival under such poor conditions, the mutated cancer cells with the stronger survival potential are gradually selected and begin to predominate within the tumor. These processes contribute to the progression of more malignant tumor phenotypes, as well as to the acquisition of resistance to radiotherapy and chemotherapy [13]. In order to characterize the changes in gene expression profiles under poor conditions, we incubated HEK293 cells under both hypoxic and iron-deficient conditions for 24 h and subsequently analyzed gene expression with oligochips. As iron deficiency can be established easily with a chelator desferrioxamine (DFO), we selected an iron-deficient model for use as an example of nutritional deficiency. Our microarray assay revealed that SSAT expression was reproducibly enhanced in both the hypoxic and DFO-treated cells (Fig. 1A). In order to confirm SSAT mRNA induction, we analyzed the mRNA levels using highly sensitive RT-PCR, using [α-$^{32}$P]dCTP. Unexpectedly, two PCR products, of 440 and 330 bp, were identified, and only the bigger fragment was induced by hypoxia and DFO, but not the smaller one. $CoCl_2$, which is frequently used as a hypoxia-mimetic agent, also induced the expression of the bigger fragment (Fig. 1B, left panel). Our DNA sequencing revealed that the smaller fragment is the wild-type SSAT and the bigger fragment is the SSAT variant. In the variant, a 110-bp segment within intron 3 was spliced in between exons 3 and 4 (Fig. 1B, right panel). In order to quantify these PCR fragments, each radioactive band was cut out from the dried gel, and then the radioactivities of the gel bands were measured with a β-counter. The relative amount of variant mRNA is represented in Fig. 1C and was assessed by dividing the cpm value of the variant fragment by that of the wild-type fragment. The mean expression levels of the variant mRNA are approximately 1.6-fold those of the wild-type in the hypoxic cells and 1.8-fold in the DFO-treated cells. If the total transcript levels are not altered, the increase in alternative mRNA splicing should prove to reduce the levels of wild-type mRNA. However, SSAT mRNA levels were not decreased, even though the variant mRNA levels increased by 7-fold that of the control. This suggests that variant mRNA does not originate from the pre-mRNA of the SSAT. Thus, we speculate that, compared to SSAT, the variant transcript may be generated and regulated by a different promoter, and thus be processed in a different way. This point remains to be clarified in a future study. To examine whether the induction of the SSAT variant occurs in other types of cells, various human cancer cell-lines were subjected to DFO or hypoxia for 16 h. The SSAT variant was inducible in four types of cells, e.g., Caki1, HT29, SiHa, and PC3, whereas it was not in three types of cells, e.g., Hep3B, MCF7, and MKN28 (Fig. 1E). Of these, Caki1 and PC3 expressed the variant in response to DFO, and HT29 and SiHa did in response to hypoxia. Therefore, the SSAT variant can be induced in various types of cells and the responses to DFO and hypoxia may depend on cell type. However, since we checked SSAT mRNAs in an experimental condition, we do not know if the SSAT variant is induced after a longer incubation even in Hep3B, MCF7, or MKN28 cells. In order to obtain clones of SSAT and its variant, the full-length SSAT cDNAs, measuring ~1 kb, were amplified using

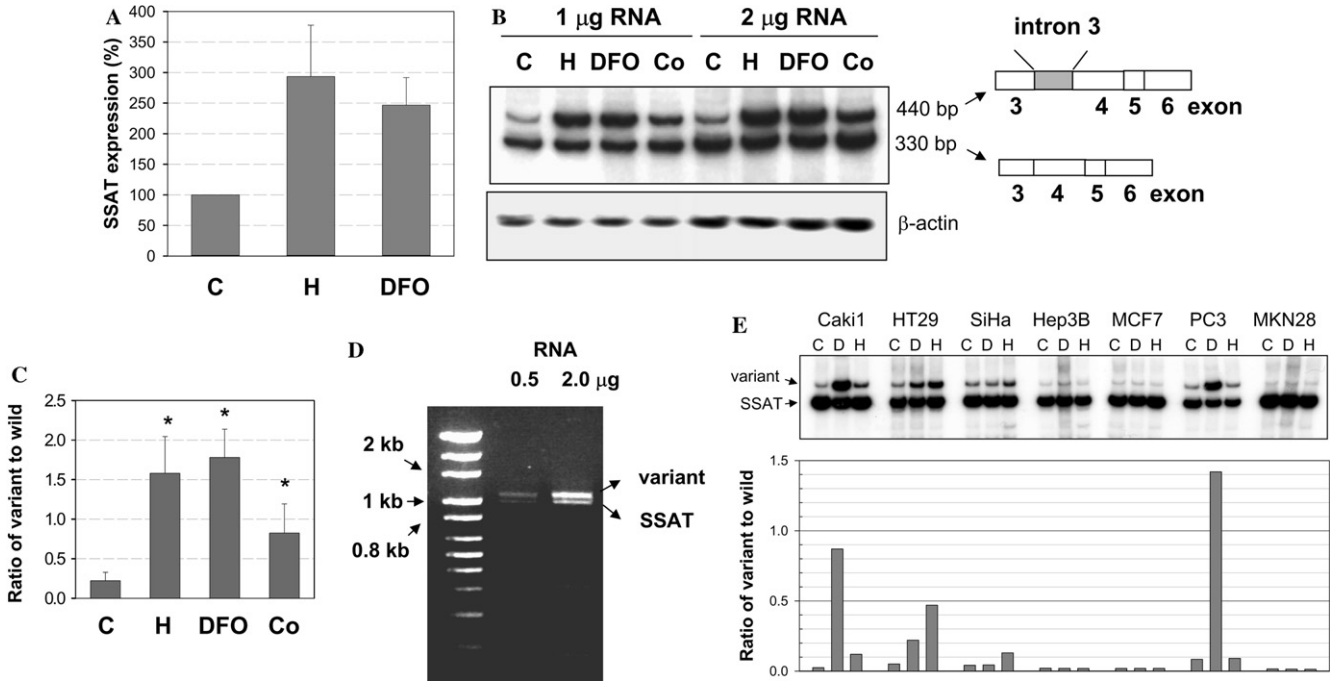


Fig. 1. Identification of an inducible splice variant of SSAT mRNA. Total RNA was extracted from HEK293 cells grown under normal (C), hypoxic (H), 130 μM desferrioxamine (DFO), or 100 μM $CoCl_2$ conditions, for 24 h. Cy3 or Cy5 dye-labeled cDNA probes were generated from total RNAs, and applied to array slides containing oligonucleotides for 11,000 human cDNAs, and the gene expression profile was analyzed using Genepix 3.0 software. Each sample was also reciprocally labeled. The data represent means + SD from three separate experiments (A). The cellular SSAT mRNA levels were analyzed via semi-quantitative RT-PCR, as described in the Materials and methods. The RNA structures of the two PCR fragments were analyzed by direct DNA sequencing and are illustrated in the right panel (B). The relative amounts of the mRNAs were calculated by dividing the cpm value of the 440 bp fragment by that of the 330 bp fragment. The data represent means + SD from three separate experiments. *$p < 0.05$ vs. the control (C). The full-length SSAT cDNAs were amplified using RT-PCR and then electrophoresed on 1.5% agarose gel (D). Various cancer cells were treated with 130 μM desferrioxamine (D) or 1% $O_2$ hypoxia (H) for 16 h, and their SSAT mRNAs were analyzed via the RT-PCR method (E). The relative amounts of SSAT mRNAs were calculated as described in (C) and the result is displayed in the figure.

RT-PCR and sequenced. DNA sequencing revealed that the variant had no alternative splicing other than the splicing-in of intron 3. We inserted both cDNA into pcDNA and HA-tag pcDNA to construct the mammalian expression vectors.

The structures and activities of the SSAT isoforms are summarized in Fig. 2. Comparison with SSAT genomic organization (GenBank No., Z14136) revealed that the cloned cDNA was derived from an alternatively spliced mRNA, which exhibits an additional 110-base segment of intron 3 (Fig. 2A). As both of the junction sites of the new exon exhibit the typical splicing junction sequence (AG/GT) [14], this splicing-in is probably a real event, but not an artifact. In this mRNA, the splicing-in results in a shift in the reading frame, and generates a new short frame and an immediate termination codon. Consequently, this alternative splicing results in the introduction of three new amino acids, Tyr-Ser-Leu, which constitutes a new C-terminus, following the amino acid $Gly^{68}$ of SSAT. This variant mRNA translates a short polypeptide of 71 amino acids, which we designated inducible short SSAT, or *is*SSAT. Compared to SSAT, *is*SSAT contains only the N-terminal half, but lacks both the acetyl-CoA binding [15] and catalytic motifs [16], both of which are essential for the enzymatic reaction of polyamine acetylation (Fig. 2B). Therefore, we expect that *is*SSAT is unable to function as a polyamine-metabolizing enzyme. Indeed, expressed *is*SSAT was found not to convert spermidine to acetylspermidine, whereas wild-type SSAT protein did (Fig. 2C).

We attempted to determine the sensitivity and specificity of *is*SSAT induction. Fig. 3 revealed that *is*SSAT mRNA was significantly induced at DFO concentrations as low as 20 μM, and that the induction was reversed by iron supplementation. Moreover, the variant was fully induced as early as 8 h after treatment with DFO. These results suggest that *is*SSAT expression is regulated both sensitively and specifically. How is *is*SSAT expression regulated? We first ruled out the possibility that the depletion of ATP is responsible for the *is*SSAT generation. Iron and oxygen deficiency may block ATP synthesis, which in turn affects transcription and RNA processing. However, the ATP levels were not changed significantly in the condition that *is*SSAT was fully induced by DFO (Fig. 3B, lower panel). Moreover, when the ATP levels were dropped by the combination of cyanide and 2-deoxy-D-glucose, *is*SSAT was slightly

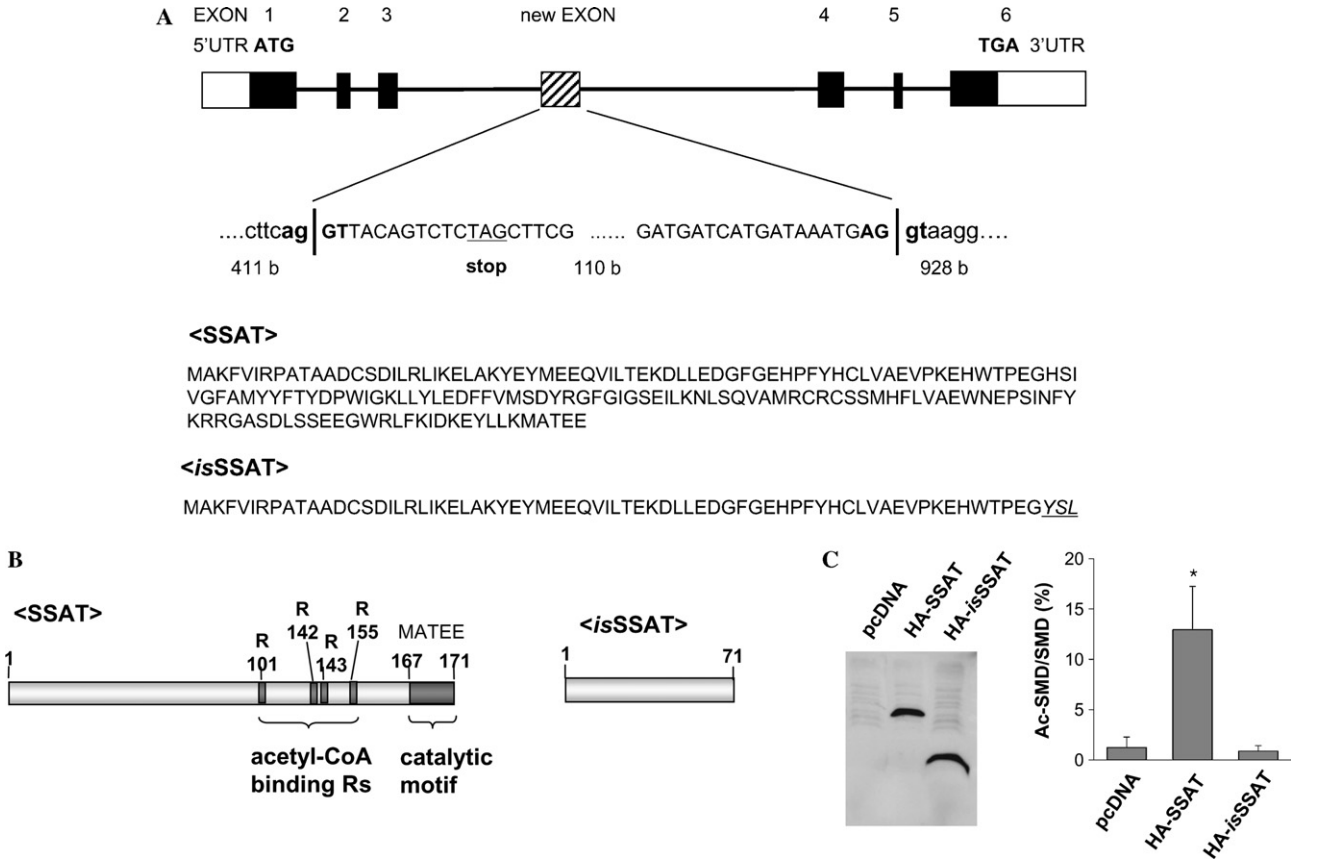


Fig. 2. Structure and enzymatic activities of SSAT isoforms. Schematic representation of an inducible isoform (*is*SSAT) compared with wild-type SSAT. A 110-base fragment within intron 3 is spliced in between exons 3 and 4, thereby causing a shift in the reading frame, and generating three new amino acids in the C-terminal end (underlined) and an early termination of translation. The junction sites of the alternative splicing and peptide sequences are represented (A). Compared to SSAT, the variant has lost all motifs for enzymatic action. The amino acids and motifs essential for enzymatic action are illustrated (B). Cells were transiently transfected with 10 μg pcDNA, pHA-SSAT, or pHA-*is*SSAT, and expression was verified utilizing Western blotting with anti-HA antibody (C, left panel). The intracellular levels of spermidine (SMD) and acetylspermidine (Ac-SMD) were analyzed via the HPLC method, as described in the Materials and methods. The results were calculated by dividing the concentration of Ac-SMD by that of SMD and represent means + SD of three separate experiments (C, right panel). $*p < 0.05$ vs. the pcDNA control.

decreased. Reversely, wild-type SSAT was significantly induced in a time-dependent manner (Fig. 3C). These results suggest that the *is*SSAT generation was not relevant to the energy status, rather the SSAT induction was. Second, we considered the possibility that hypoxia-inducible factor 1alpha (HIF-1α) upregulates *is*SSAT, as hypoxia, DFO, and $CoCl_2$ are all known to be strong HIF-1α inducers, and HIF-1α is a master transcription factor in the upregulation of 60 varieties of hypoxia-inducible genes. Normally, HIF-1α is degraded by the von Hippel–Lindau protein (pVHL), a component of the E3 ubiquitin ligase protein complex. Hypoxia and the HIF-1α inducers facilitate the escape of HIF-1α from pVHL binding and cause the stabilization of HIF-1α [17]. Therefore, HIF-1α is not regulated in the pVHL-null 786-O cells, which is why this cell-line is commonly used to identify HIF-1α regulated genes [18]. However, *is*SSAT mRNA was induced by DFO, even in the 786-O cells (Fig. 3C). Moreover, *is*SSAT was also induced in HIF-1α (−/−) MEF cells (data not shown). These results indicate that HIF-1α is not responsible for the regulation of *is*SSAT. On the other hand, oxygen and iron are prone to the generation of reactive oxygen species [19]. Conversely, hypoxia and DFO can ameliorate oxidative stress and shift the intracellular redox state to antioxidant status [20]. In order to determine whether *is*SSAT expression depends on redox state, we treated cells with a prooxidant $H_2O_2$ or with the antioxidants trolox and *N*-acetyl cysteine. $H_2O_2$ was not observed to reverse the DFO effect, and antioxidants were not observed to mimic the DFO effect (Fig. 3D), which suggests that *is*SSAT expression is independent of redox state. In the present study, we were also unable to clarify the regulatory mechanism of *is*SSAT expression, which remains to be determined.

Recently, Ichimura et al. [21] reported that SSAT mRNA expression could be induced in HeLa S3 cells by X-ray irradiation. After 3 days of irradiation with 5 Gy of X-rays, mRNA levels had increased up to three times those of the unirradiated control, but this effect

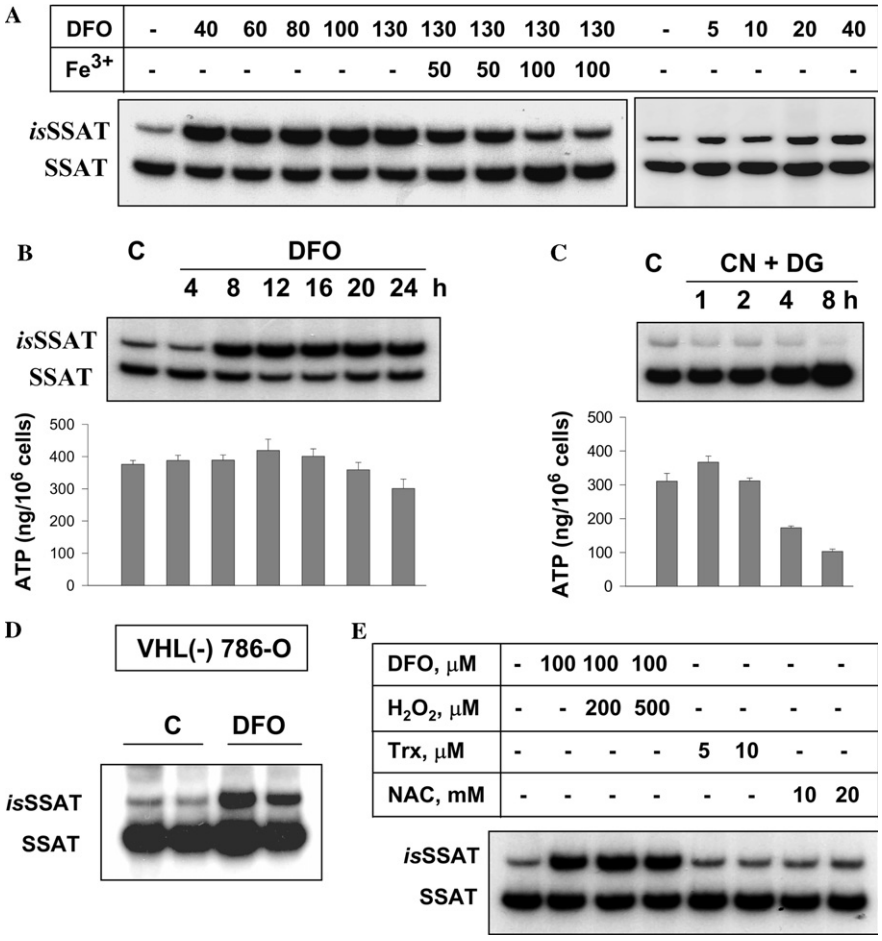


Fig. 3. Regulation of *is*SSAT expression. HEK293 cells were incubated with various desferrioxamine (DFO) concentrations in the absence or presence of $FeCl_3$ for 24 h (A). HEK293 cells were treated with 100 μM DFO for various incubation times (B). HEK293 cells were treated with 5 mM potassium cyanide (CN) and 5 mM 2-deoxy-D-glucose (DG) for various incubation times (C). 786-O cells were incubated with 100 μM DFO for 24 h (D). HEK293 cells were co-treated with DFO and $H_2O_2$, or treated with trolox (Trx) and *N*-acetyl cysteine (NAC) for 24 h (E). SSAT and *is*SSAT mRNAs were analyzed via RT-PCR, and ATP levels were measured by the bioluminescence method, as described in Materials and methods. The detailed conditions are indicated above each figure.

was not induced by hypoxia or DFO treatment in our study. This discrepancy may be attributable to the different experimental conditions used in the respective studies, including differences in stimulus and long-term incubation. In addition to SSAT mRNA, they determined that a longer SSAT mRNA had also been induced by X-rays. According to this report, the longer variant appears identical to *is*SSAT, as the variant possessed 110 more bases between exons 3 and 4 of the SSAT gene. However, they did not delineate the role of the SSAT variant in response to X-ray irradiation. In the present study, in order to determine the functional role of *is*SSAT, we constructed cell-lines which stably expressed either HA-tagged SSAT or untagged *is*SSAT. As described in the Materials and methods, we produced an antibody against *is*SSAT and confirmed that this antibody was sufficient for the detection of ectopically expressed *is*SSAT protein. Thus, we are able to express untagged *is*SSAT and to determine its levels with this antibody. However, this antibody was not sufficiently sensitive to detect endogenous *is*SSAT (data not shown). Unexpectedly, this antibody proved to be unreactive to SSAT protein, although SSAT contains almost the entire length of *is*SSAT. In order to determine the expression levels, we were compelled to express HA-tagged SSAT. In transfected cell-lines, we confirmed that either *is*SSAT or HA-SSAT was expressed, as shown in Fig. 4A. As the SSAT protein is actively destroyed by the proteasome, it is found to be present only in very small amounts. Therefore, after we blocked the proteasomal degradation with MG132, we were able to verify that *is*SSAT and HA-SSAT had been expressed adequately.

What, then, is the role of *is*SSAT? Considering it is induced under unfavorable conditions, it may contribute to either growth arrest or cell death. Conversely, it is possible that it functions as a defensive molecule, fostering cell survival. In order to answer this question,

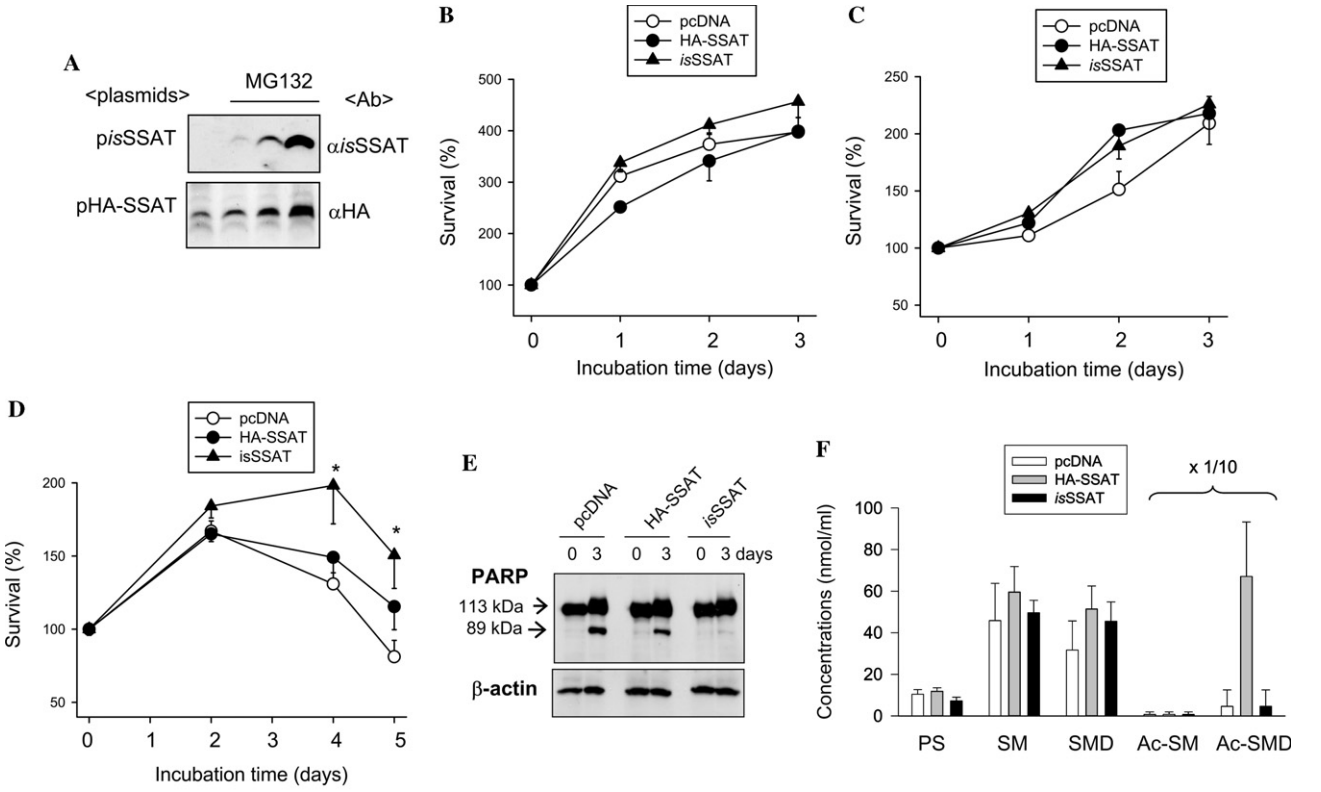


Fig. 4. Roles of *is*SSAT in cell growth and survival. HEK293 cells were transfected with pcDNA, pHA-SSAT, or p*is*SSAT, and selected with G418. After cells were treated with MG132 or vehicle (DMSO) for 6 h, the expression of *is*SSAT or HA-SSAT proteins was verified via Western blotting with anti-*is*SSAT or anti-HA antibodies (A). The stable cell-lines were grown in DMEM containing 10% serum (B). The cell-lines were grown in media containing 0.1% serum (C). The cell-lines were grown in media containing 10% serum and 100 μM DFO (D). The number of viable cells was estimated via MTT assays, as described in the Materials and methods. $*p < 0.05$ vs. the pcDNA group. Cells, grown with DFO for 3 days, were then harvested in lysis buffer, as described in Materials and methods, and poly(ADP–ribose) polymerase and β-actin in samples were detected using their specific antibodies. One hundred thirteen and eighty-nine kilodalton bands represent intact and cleaved PARP proteins, respectively (E). The intracellular levels of polyamines in the stable cell-lines were analyzed via HPLC. The identification and concentration of each polyamine species were evaluated in reference to retention time and the peak area of the corresponding authentic compound, as shown in supplementary material 2. PS, putrescine; SM, spermine; SMD, spermidine; Ac-SM, acetylspermine; Ac-SMD, acetylspermidine. Each bar represents the means + SD of three separate experiments (F).

we first attempted to determine whether *is*SSAT affects cell growth under favorable conditions in which serum, oxygen, and iron are enriched. We determined that there are no differences with regard to cell proliferation for 3 days among the three cell-lines (Fig. 4B). Second, we removed the serum from the medium, but the proliferation rates of all cell-lines were found to decelerate to a similar degree (Fig. 4C). Third, we attempted to ascertain whether *is*SSAT affects cell death under unfavorable conditions. All of the cell-lines grew slowly until the second day after DFO treatment. After 4 days, the viabilities of the control and HA-SSAT cell-lines were observed to decrease abruptly. However, the viability of the *is*SSAT cell-line was much higher that those of the others (Fig. 4D). As a marker for apoptotic death, we measured poly(ADP–ribose) polymerase (PARP) cleavage [22]. PARP was not cleaved in the *is*SSAT cell-line, but was cleaved in all of the other cell-lines (Fig. 4E). These results suggest that *is*SSAT may exert a protective function in apoptotic cell death. How, then, does *is*SSAT ameliorate cell death? As it appears to possess no catalytic motif, we expect that it has no effect on the total amount and composition of polyamines. Indeed, the polyamine levels in the *is*SSAT cell-line were equal to those observed in the control cell-line (Fig. 4F). Even in the HA-SSAT cell-line, the intracellular polyamine levels, except for that of acetylspermidine, were not significantly changed. Polyamine metabolism appears to readjust, thereby maintaining polyamine level homeostasis in the stable cell-lines [23]. This result suggests that polyamine levels were essentially irrelevant to the protective effects of *is*SSAT, which may involve direct interaction with some apoptotic process. The mechanism underlying the *is*SSAT effect is currently the focus of another study.

In the present study, microarray analysis revealed that the levels of SSAT mRNAs increased under hypoxic or iron-deficient conditions. We determined that this upregulation of SSAT was attributable to the specific induction of a SSAT variant, but not due to wild-type induction. Here, we designated the SSAT

isoform derived from the variant mRNA "*is*SSAT." *is*SSAT did not appear to participate in polyamine metabolism, due to the loss of all of the motifs essential for the enzymatic reaction. However, it is likely to play an important role in cell survival under poor conditions, via its preventive effects on apoptotic death. Considering its induction under unfavorable conditions and protective effects on cell death, it may contribute to the progression of tumors of a more malignant phenotype under unfavorable conditions, as well as to the acquisition of resistance to radiotherapy and chemotherapy. If this is, indeed, the case, it is apparent that the inhibition of *is*SSAT may constitute a novel strategy for the treatment of cancer, and further study into the mechanisms underlying the regulation of *is*SSAT expression is clearly warranted.

## Acknowledgment

This work was supported by a Korea Research Foundation Grant (KRF-2003-015-200053).

## Appendix A. Supplementary data

Supplementary data associated with this article can be found, in the online version, at doi:10.1016/j.bbrc.2005.03.121.

## References

[1] R.A. Casero Jr., A.E. Pegg, Spermidine/spermine *N*1-acetyltransferase—the turning point in polyamine metabolism, FASEB J. 7 (1993) 653–661.
[2] T. Thomas, T.J. Thomas, Polyamines in cell growth and cell death: molecular mechanisms and therapeutic applications, Cell Mol. Life Sci. 58 (2001) 244–258.
[3] J.L. Urdiales, M.A. Medina, F. Sanchez-Jimenez, Polyamine metabolism revisited, Eur. J. Gastroenterol. Hepatol. 13 (2001) 1015–1019.
[4] L. Xiao, P. Celano, A.R. Mank, C. Griffin, E.W. Jabs, A.L. Hawkins, R.A. Casero Jr., Structure of the human spermidine/spermine *N*1-acetyltransferase gene (exon/intron gene organization and localization to Xp22.1), Biochem. Biophys. Res. Commun. 187 (1992) 1493–1502.
[5] C.S. Coleman, A.E. Pegg, Proteasomal degradation of spermidine/spermine *N*1-acetyltransferase requires the carboxyl-terminal glutamic acid residues, J. Biol. Chem. 272 (1997) 12164–12169.
[6] C.W. Porter, B. Ganis, P.R. Libby, R.J. Bergeron, Correlations between polyamine analogue-induced increases in spermidine/spermine *N*1-acetyltransferase activity, polyamine pool depletion, and growth inhibition in human melanoma cell lines, Cancer Res. 51 (1991) 3715–3720.
[7] P. Vaupel, F. Kallinowski, P. Okunieff, Blood flow, oxygen consumption and tissue oxygenation of human tumors, Adv. Exp. Med. Biol. 277 (1990) 895–905.
[8] T. Henning, M. Kraus, M. Brischwein, A.M. Otto, B. Wolf, Relevance of tumor microenvironment for progression, therapy and drug development, Anticancer Drugs 15 (2004) 7–14.
[9] J.M. Brown, W.R. Wilson, Exploiting tumour hypoxia in cancer treatment, Nat. Rev. Cancer 4 (2004) 437–447.
[10] Y.S. Chun, K.H. Lee, E. Choi, S.Y. Bae, E.J. Yeo, L.E. Huang, M.S. Kim, J.W. Park, Phorbol ester stimulates the nonhypoxic induction of a novel hypoxia-inducible factor 1alpha isoform: implications for tumor promotion, Cancer Res. 63 (2003) 8700–8707.
[11] S. Vujcic, M. Halmekyto, P. Diegelman, G. Gan, D.L. Kramer, J. Janne, C.W. Porter, Effects of conditional overexpression of spermidine/spermine *N*1-acetyltransferase on polyamine pool dynamics, cell growth, and sensitivity to polyamine analogs, J. Biol. Chem. 275 (2000) 38319–38328.
[12] R.S. Bindra, P.M. Glazer, Genetic instability and the tumor microenvironment: towards the concept of microenvironment-induced mutagenesis, Mutat. Res. 569 (2005) 75–85.
[13] M. Hockel, P. Vaupel, Biological consequences of tumor hypoxia, Semin. Oncol. 28 (2001) 36–41.
[14] S.M. Mount, A catalogue of splice junction sequences, Nucleic Acids Res. 10 (1982) 459–472.
[15] C.S. Coleman, H. Huang, A.E. Pegg, Structure and critical residues at the active site of spermidine/spermine-*N*1-acetyltransferase, Biochem. J. 316 (1996) 697–701.
[16] C.S. Coleman, H. Huang, A.E. Pegg, Role of the carboxyl terminal MATEE sequence of spermidine/spermine *N*1-acetyltransferase in the activity and stabilization by the polyamine analog *N*1,*N*12-bis(ethyl)spermine, Biochemistry 34 (1995) 13423–13430.
[17] Y.S. Chun, M.S. Kim, J.W. Park, Oxygen-dependent and -independent regulation of HIF-1alpha, J. Kor. Med. Sci. 17 (2002) 581–588.
[18] Y. Jiang, W. Zhang, K. Kondo, J.M. Klco, T.B. St Martin, M.R. Dufault, S.L. Madden, W.G. Kaelin Jr., M. Nacht, Gene expression profiling in a renal cell carcinoma cell line: dissecting VHL and hypoxia-dependent pathways, Mol. Cancer Res. 1 (2003) 453–462.
[19] C.C. Winterbourn, Toxicity of iron and hydrogen peroxide: the Fenton reaction, Toxicol. Lett. 82 (1995) 969–974.
[20] R.J. Rothman, A. Serroni, J.L. Farber, Cellular pool of transient ferric iron, chelatable by deferoxamine and distinct from ferritin, that is involved in oxidative cell injury, Mol. Pharmacol. 42 (1992) 703–710.
[21] S. Ichimura, M. Nenoi, K. Mita, K. Fukuchi, Accumulation of spermidine/spermine *N*1-acetyltransferase and alternatively spliced mRNAs as a delayed response of HeLa S3 cells following X-ray irradiation, Int. J. Radiat. Biol. 80 (2004) 369–375.
[22] M. Tewari, L.T. Quan, K. O'Rourke, S. Desnoyers, Z. Zeng, D.R. Beidler, G.G. Poirier, G.S. Salvesen, V.M. Dixit, Yama/CPP32 beta, a mammalian homolog of CED-3, is a CrmA-inhibitable protease that cleaves the death substrate poly(ADP–ribose) polymerase, Cell 81 (1995) 801–809.
[23] H.M. Wallace, A.V. Fraser, A.A. Hughes, A perspective of polyamine metabolism, Biochem. J. 376 (2003) 1–14.